2018 European Control Conference (ECC)
June 12-15, 2018. Limassol, Cyprus

Saving Energy by Predictive Supply Air Shutoff for Pneumatic Drives*

Adrian Raisch[1], Steffen Hülsmann[2], and Oliver Sawodny[1]

***Abstract*— Pneumatic drives are a widespread drive technology with generally large energy saving potentials. Besides a proper sizing of the drive, an optimized operation can reduce energy intake of a pneumatic drive strongly. In this paper, we consider the optimal control of a pneumatic cylinder actuated by a switching valve. We present an offline computed feedforward control solution and an online control strategy. The offline control strategy delivers the energy optimal control of the cylinder. To enhance the robustness and to reduce the necessary implementation effort, we then present a novel online control strategy, employing a model-based online prediction of the system behavior. The two control concepts are analyzed and compared in simulation and experiment, where our experimental results reveal a reduction of the compressed air intake by about one half compared to a standard switching control strategy.**

I. Introduction

Pneumatic drives are widely used in industry to perform motion tasks. The most common application scenarios for pneumatic cylinders are moving, lifting, or clamping work pieces while being controlled by a switching valve. In those applications, the standard control strategy used for pneumatic drives is a simple switching between pressurizing and venting the cylinder chambers. However, this leads to a possibly large waste of energy as the cylinder is always pressurized to the supply pressure level and the energy consumption is then a consequence of a (conservative) cylinder sizing process.

Due to the large saving potentials arising in the field of pneumatic drives, energy saving measures for those have been an active field of research over the past years. In the first step, this includes the sizing of pneumatic drives. In [1], the optimal design of pneumatic servo drives is investigated, while [2] considers the sizing for end-to-end motion purposes. For systems already dimensioned, different energy saving potentials of pneumatic drives are investigated in literature [3], [4], [5]. The third focus relies on the field of control strategies – of servo systems [6], [7], and in the case of switching valves [8], [9], [10].

In this paper, we consider a planar end-to-end motion steered by a switching valve. An example for such motion tasks is depicted in Fig. 1, where the test bench used is shown. The pneumatic cylinder is driven from end stop to end stop by fully inflating and deflating its chambers. An exemplary time plot of pressure levels, position and compressed air usage corresponding to this standard actuation szenario are illustrated in Fig. 2. Starting at the position $s = 0$ with absolute chamber pressures of $p_{\mathrm{A}} = 1\mathrm{bar}$ and $p_{\mathrm{B}} = 7\mathrm{bar}$, the chamber A is fully inflated, while B is deflated. The overall compressed air consumption, the measure for the energy intake, yields 2.49 standard liters – an amount with a large savings potential as we will later see.

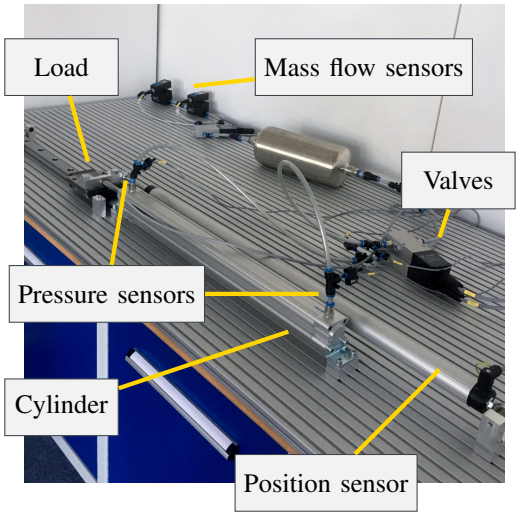

Fig. 1. Test bench for validation and experiments used in this contribution.

The motion task considered in this paper is characterized by a load mass m, transition time $t_{\mathrm{f}} - t_0$, and transition length s_{f}. We furthermore assume that the considered drive is somehow oversized, meaning it fulfills the motion task ahead of time, or its dynamics are restricted by a throttle. This gives us the opportunity to utilize control strategies for reducing the energy intake. We will later discuss and apply two control strategies to address this objective.

The remainder of this paper is organized as follows: In Section II, a physical model of the drive system is given and validated. Section III explains the problem setup in detail and presents the strategies we are investigating. Those measures are then applied to the test bench in Section IV and compared to one another. Drawbacks and benefits are discussed before the paper is closed with conclusions in Section V.

II. System Model

In this section a mathematical dynamical model of a pneumatic cylinder as depicted in Fig. 3 is described. We divide the modeling into the two parts of fluid dynamics and motion dynamics as presented in the following.

*This work is supported by the German Federal Ministry for Economic Affairs and Energy under Grant 03ET1385B. The work is part of EnAP-project (www.enap-projekt.de): Anwenderorientierter Einsatz energieffizienter Antriebstechnik in der Produktion (engl.: User oriented use of energy-efficient drive technology in production).

[1]Adrian Raisch and Oliver Sawodny are with the Institute for System Dynamics, University of Stuttgart, D-70563 Stuttgart, Germany. {raisch, sawodny}@isys.uni-stuttgart.de

[2]Steffen Hülsmann is with Festo AG & Co. KG, Ruiter Strasse 82, D-73734 Esslingen, Germany. steffen.huelsmann@festo.com

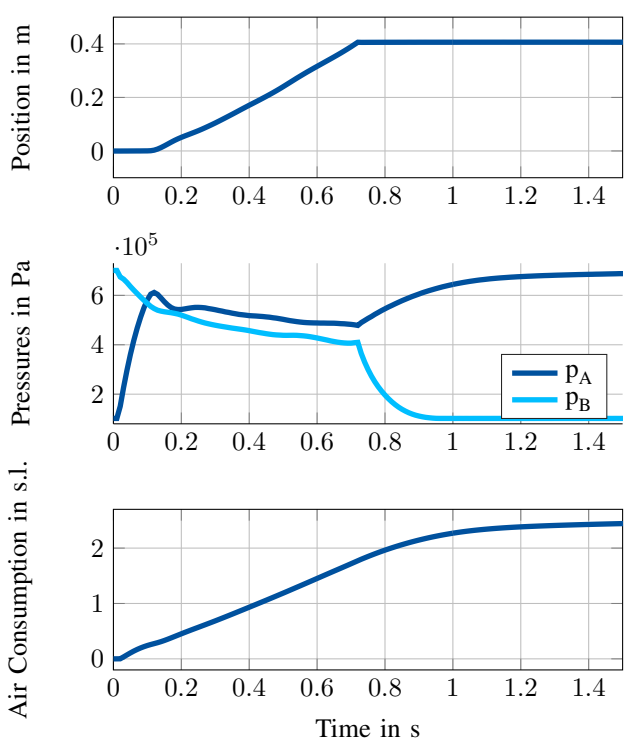

Fig. 2. Measured time behavior for a standard switching control. The chamber A is fully inflated from 1bar to 7bar, while chamber B is deflated. The overall compressed air consumption in this case is 2.49 standard liters.

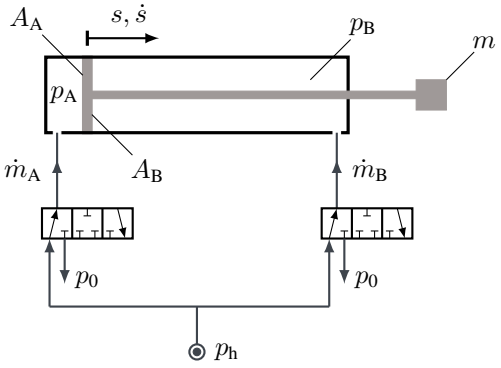

Fig. 3. Sketch of a mechanical cylinder for motion tasks in abstracted form. The indices A and B correspond to the two cylinder chambers with their respective pressures, mass inflows and areas.

A. Pressure Dynamics

The dynamics of the fluid inside the cylinder chambers – we consider air to be the working fluid – are assumed to undergo a polytropic process with the polytropic coefficient n. Neglecting temperature changes, the temperature T is taken as a constant. The dynamics of the pressures p_A, p_B inside the chambers A and B is then described as [11], [12], [13]

$$\dot{p}_{A,B} = \frac{n}{V_{A,B}(s)}(RT\dot{m}_{A,B} - \dot{V}_{A,B}(\dot{s})p_{A,B}). \tag{1}$$

Here, R is the specific gas constant, $V_{A,B}$ the volume of the chambers depending on the piston position s and dead volumes $V_{A,B}^{dead}$, and $\dot{V}_{A,B}$ represents the change of the two chamber's volumes corresponding to the piston velocity $\dot{s}$.

Assuming the valves to behave like a throttle, the mass flows $\dot{m}_A$, $\dot{m}_B$ through them can be described according to ISO 6358 [14] using the {C,b}-method by

$$\dot{m}_{A,B} = \rho p_h C \Psi(q,b) u_{A,B}, \tag{2}$$

where ρ is the density of air, p_h the upstream pressure, C is the sonic conductance, $\Psi(q,b)$ is the flow function, and u is the control input. For 3/3-switching valves – having the three states inflating, closed, and deflating – the control signal can take the discrete values $u \in \{1, 0, -1\}$. The flow function Ψ originates from an elliptical approximation of the flow capacity [15]. For the pressure ratio q of downstream pressure p_l and upstream pressure p_h, i.e. $q = \frac{p_l}{p_h}$, and the critical pressure ration b, the flow function is given by

$$\Psi(q,b) = \begin{cases} 1, & q < b \\ \sqrt{1 - (\frac{q-b}{1-b})^2}, & q \geq b \end{cases}. \tag{3}$$

B. Motion Dynamics

The kinetic behavior of the cylinder is described by the Newton's equations for the piston position s:

$$m\ddot{s} = (p_A A_A - p_B A_B - p_0(A_A - A_B) - F_F(\dot{s})). \tag{4}$$

The mass m contains the the mass of the rod as well as the load mass. The piston areas on the two sides are termed A_A and A_B and the ambiance pressure is denoted by p_0. We furthermore assume the motion dynamics to be friction afflicted by a friction force $F_F(\dot{s})$. This friction force, is modeled as a combination of Coulomb and viscous friction:

$$F_F(\dot{s}) = f_c \operatorname{sign}(\dot{s}) + f_v \dot{s} \tag{5}$$

with the friction coefficients f_c and f_v.

C. Overall Model

Combining the previously introduced relations (1)-(5), the system can be rewritten in the more compact form

$$\dot{x} = f(x,u) \tag{6}$$

with the state vector

$$x = \begin{bmatrix} s & \dot{s} & p_A & p_B \end{bmatrix}^T, \tag{7}$$

system input

$$u = \begin{bmatrix} u_A & u_B \end{bmatrix}^T, \tag{8}$$

and the nonlinear right hand side according to the dynamics as described in (1)-(5).

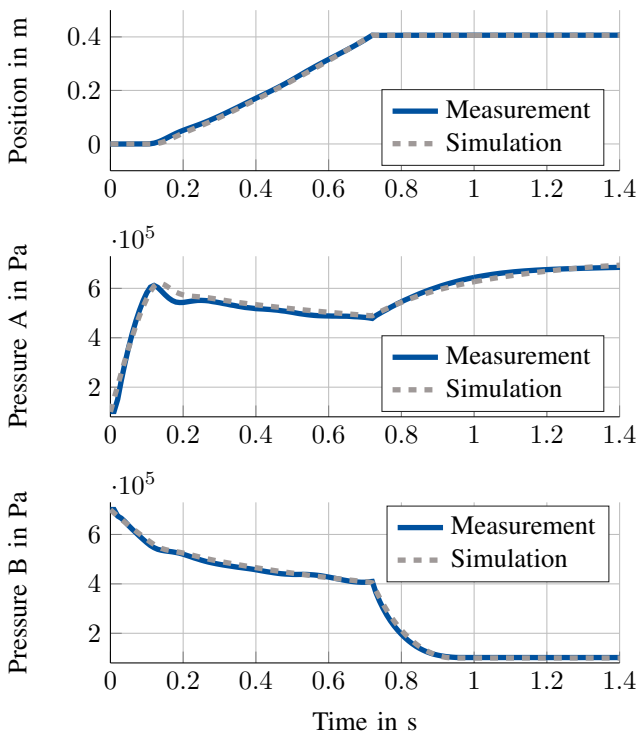

Fig. 4. Comparison of Simulation and Measurement. The physical behavior of system (measurements in blue color) is matched well by the simulative system model (gray, dashed).

D. Model Validation

Before optimizing the behavior of the system, the friction parameters and valve characteristics have to be identified. For validation purposes, Fig. 4 gives a comparison of the resulting simulative and experimental behavior. Obviously, the physical behavior of the system is matched quite well by the system description (6).

III. Control Problem and Proposed Solutions

A. Overall Setup

Our overall goal is to minimize the compressed air intake of a pneumatic cylinder for a given motion task, i.e.

$$\min \int_{T_0}^{T_\mathrm{f}} \dot{m}_\mathrm{A}^+(x,u) + \dot{m}_\mathrm{B}^+(x,u)\mathrm{d}t \tag{9a}$$

$$\text{s.t.} \quad \dot{x} = f(x,u) \tag{9b}$$

$$x(T_0) = x_0 \tag{9c}$$

$$g(x(T_\mathrm{f})) \leq 0 \tag{9d}$$

Here, $\dot{m}_\mathrm{A}^+$ and $\dot{m}_\mathrm{B}^+$ represent the compressed air intake of the cylinder meaning only positive mass flows. The initial condition is described by (9c) and the terminal state is not fully specified (9d).

In following we compare different strategies for achieving this goal. The general motion task considered in this paper was already described in the previous modeling section and as a specific example we regard a displacement of a mass of 2kg by 0.4m within 1s. The supply air is at a pressure level of 7bar and a cylinder with a diameter of 32mm is used to fulfill the motion task. At the stroke end, the cylinder reaches an end stop and thus the only requirement on the terminal condition $g(x(T_\mathrm{f}))$ in our case is that $s(T_\mathrm{f}) = 0.4$. In the following, we assume this setup to be a feasible optimization problem, meaning the supply pressure is high enough such that the cylinder can fulfill the motion task. This described scenario corresponds to the previously illustrated trajectories in Fig. 4.

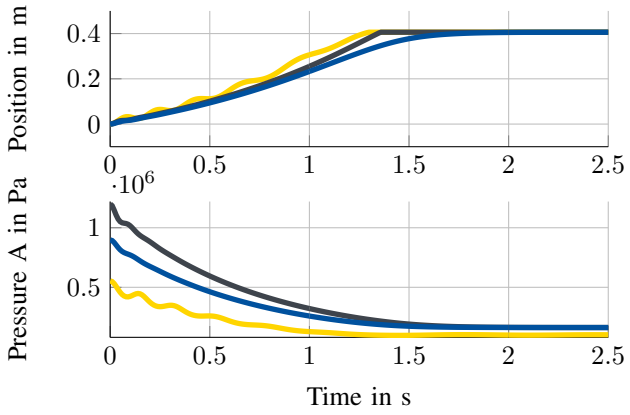

Fig. 5. Simulated system behavior with only expansion and no mass inflow into the system. The oscillation of the yellow line is a consequence of the absence of friction. The other scenarios incorporate friction and illustrate initial pressures where the end stop is just reached (blue line) and where $p_\mathrm{A}(t_0) = 12\mathrm{bar}$. In all cases, the transition time exceeds the asked 0.8s.

B. Exploitation of expansion energy

Before introducing an optimized control strategy for the switching valve, we take a look at the physical effect that underlies the proposed energy saving measures: the expansion of preloaded air. We briefly consider the potential arising from the expansion in a polytropic process, as well as its limitations of the pure use of expansion energy in the case of motion tasks. When shutting off the supply air of a pneumatic cylinder, where the expanding chamber is under a certain preload, the expansional energy of compressed air comes into effect. For a polytropic process – which we assume in this paper – the relation

$$p(t_1)V(t_1)^n = p(t_2)V(t_2)^n \tag{10}$$

holds for any time instances t_1, t_2. When assuming no friction, one can calculate the necessary initial pressure for a given expansion. For chamber A of the presented system, this results in

$$p_\mathrm{A}(t_1) = p_\mathrm{A}(t_2)\left(\frac{V_\mathrm{A}^\mathrm{dead} + A_\mathrm{A}s(t_2)}{V_\mathrm{A}^\mathrm{dead}}\right)^n. \tag{11}$$

In case of the here considered (simplified) friction model (5), the piston will come to a stop as soon as

$$p_\mathrm{A}(t) = \frac{f_\mathrm{c}}{A_\mathrm{A}} + p_0 = p_{\mathrm{A,min}}. \tag{12}$$

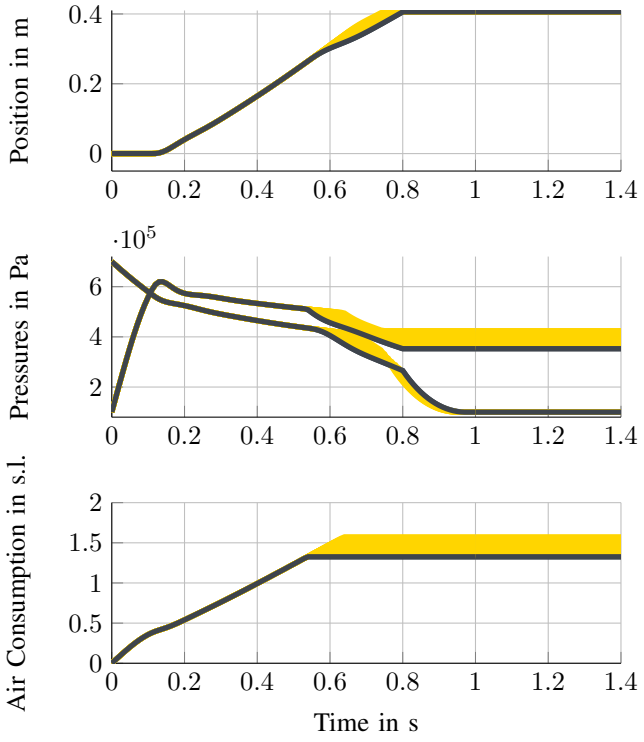

Fig. 6. Simulation of the results of an optimal supply air shutoff. The consequences of a longer inflation of the chamber A are illustrated in yellow color: The longer the inflating process is active, the shorter the transition time becomes, and the larger is the pressure at stroke end.

When using $p_{\mathrm{A}}(t_2) = p_{\mathrm{A,min}}$ in (11), this leads to the minimal initial pressure in chamber A, such that the cylinder will just reach the end stop. However, (11) gives no information on the duration $t_2 - t_1$ this process will take. In a simulative illustration of this process in Fig. 5, we give an example of the two cases just mentioned (yellow line without friction, and blue line with friction in Fig. 5), and additionally illustrate the behavior if $p_{\mathrm{A}}(t_1) = 12\mathrm{bar}$ – a standard maximum pressure value for many pneumatic tubes and cylinder (gray line in Fig. 5).

The time behavior in Fig. 5 reveals the long time duration for reaching the end stop. In all three cases, the demanded transition time of $0.8\mathrm{s}$ obviously exceeded. The oscillations in the simulative example without friction is a consequence of the then undamped mechanical system. As mentioned before, the time period for reaching the end stop is unknown, just as the necessary time to preload chamber A with the corresponding initial pressure.

Hence we can conclude the necessity of both: expansion and displacement coming from the air supply in order to save energy and maintain given cycle times. This leads to an optimization problem for switching the control valve, being discussed in the following.

C. Optimized supply air shutoff

The first technically realizable measure we consider in this paper is a feed-forward control of the state of the control valve. We consider the case of switching valves for inflating and deflating of the cylinder chambers. For the process and the control we make the following assumptions:

(A1) In order to avoid a valve chattering, we only allow one switch of the valve position u_{A} from $u_{\mathrm{A}} = 1$ to $u_{\mathrm{A}} = 0$.

(A2) Chamber B is deflated for the whole process: $u_{\mathrm{B}} \equiv -1$.

(A3) The supply pressure is always larger than the pressure in chamber A: $p_{\mathrm{h}} > p_{\mathrm{A}}(t)\ \forall t$.

Under these assumptions, we can make the following conclusions for the optimization problem (9a) and the corresponding cost function:

From (A2) it follows that $m_{\mathrm{B}}^{+}(x,u) \equiv 0$, since then – according to (2) – the mass flow $m_{\mathrm{B}}(t)$ into chamber B is non-positive:

$$\dot{m}_{\mathrm{B}} = \underbrace{\rho p_{\mathrm{B}} C}_{>0} \underbrace{\Psi\left(\frac{p_0}{p_{\mathrm{B}}}, b\right)}_{\geq 0} \underbrace{u_{\mathrm{B}}}_{=-1} \leq 0. \tag{13}$$

Further, we know that $m_{\mathrm{A}}^{+}(x,u) = 0 \Leftrightarrow u_{\mathrm{A}} = 0$, since from (A3) it follows that $\Psi(\frac{p_{\mathrm{A}}}{p_{\mathrm{h}}}, b) > 0$ and hence

$$\dot{m}_{\mathrm{A}} = \underbrace{\rho p_{\mathrm{h}} C \Psi\left(\frac{p_{\mathrm{A}}}{p_{\mathrm{h}}}, b\right)}_{>0} u_{\mathrm{A}}. \tag{14}$$

Remark 1. *For two different switching times of the control valve t_1, t_2 with $T_f \geq t_2 > t_1 \geq T_0$, the mass flow J_2 into chamber A under usage of the switching time t_2 is strictly greater than the mass flow J_1 into chamber A under the employment of the switching time t_1.*

Proof. Calculating J_2 yields

$$J_2 = \int_{T_0}^{T_{\mathrm{f}}} m_{\mathrm{A}}^{+}(x,u)\mathrm{d}t \tag{15}$$

$$= \underbrace{\int_{T_0}^{T_1} m_{\mathrm{A}}^{+}(x,u)\mathrm{d}t}_{=J_1} + \underbrace{\int_{T_1}^{T_2} m_{\mathrm{A}}^{+}(x,u)\mathrm{d}t}_{>0} + \underbrace{\int_{T_2}^{T_{\mathrm{f}}} m_{\mathrm{A}}^{+}(x,u)\mathrm{d}t}_{=0} \tag{16}$$

$$> J_1. \tag{17}$$

□

Considering these properties, we can rewrite the optimization problem (9a)-(9d) by the minimization of the switching time T_{s}

$$\begin{aligned} \min \quad & T_{\mathrm{s}} && \text{(18a)}\\ \text{s.t.} \quad & \dot{x} = f(x,u) && \text{(18b)}\\ & x(T_0) = x_0, \quad g(x(T_{\mathrm{f}})) \leq 0 && \text{(18c)}\\ & u = \begin{cases} \begin{bmatrix} 1 & -1 \end{bmatrix}^{\mathrm{T}}, & t < T_{\mathrm{s}} \\ \begin{bmatrix} 0 & -1 \end{bmatrix}^{\mathrm{T}}, & t \geq T_{\mathrm{s}} \end{cases} && \text{(18d)} \end{aligned}$$

with the switching time T_{S}. As the only decision variable left in (18a)-(18d) is the switching time of the valve position,

the optimal control problem (9a)-(9d) has become a one-dimensional constrained optimization problem having structural similarites with time optimal control problems, where – in case of bang-bang-solutions – also switching points are to be determined [16], [17].

The solution's time behavior for the given motion task is illustrated in Fig. 6 together with a variation of the switching time: The gray line corresponds to the energy optimal switching time, where the end stop is just reached at 0.8s. Increasing the switching time results in a faster transition at the cost of an increasing air intake. Furthermore, an increased switching time corresponds to a higher pressure of chamber A at the stroke end and thus a larger robustness against uncertainties.

D. Supply Air shutoff via end stop prediction

The previously described supply air shutoff is a strict feed-forward control with an optimized switching time for the control valve. However, this feed-forward control comes with the typical drawbacks of non-feed-back structures: in case of model uncertainties or parameter changes – e.g. the friction behavior could change over time, or a leakage in the system could influence the system – the pure feed-forward control will mismatch the planned behavior. In order to keep our system robust against those uncertainties we want to shift the valve switching from an offline planned process to an online decision for the supply air shutoff by a model-based prediction as described in the following.

The key idea is to calculate the point for shutting of the supply air online. During operation, in each time instance t_i, do the following:

1) Reconstruct the current system state $\hat{x}(t_i)$ and determine remaining time for transition $\Delta T = T_\mathrm{f} - t_i$.
2) Perform a forward simulation of the system (6) with $u = \begin{bmatrix} 0 & -1 \end{bmatrix}^\mathrm{T}$, i.e. the case where the supply air for chamber A is shut off and chamber B is further deflated. Start the simulation at the current system state $\hat{x}(t_i)$ and simulate for the time span ΔT.
3) In case where the motion task will be fulfilled according to the current prediction, shut off the supply air by choosing $u_\mathrm{A} = 0$. Otherwise continue to inflate chamber A ($u_\mathrm{A} = 1$). To increase the robustness of the control scheme, the condition for reaching the terminal state should be restrained to a time before T_f.

The controlled system structure under this predictive control strategy is sketched as a block diagram in Fig. 7. Note that the practical realization of the state reconstruction logically requires sensors. On our test bench, we measured the chamber pressures and the position and use this information to reconstruct the system's state $\hat{x}(t)$.

Remark 2 (Comparison to an MPC scheme)**.** *If we compare the proposed predictive control strategy to the use of a classical MPC-scheme, we can observe that the outcome is the same in our case: A MPC-scheme optimizes the switching time T_s in each time instance and applies $u_A = 1$ as long as $t < T_s$. As soon as the switching time is reached,*

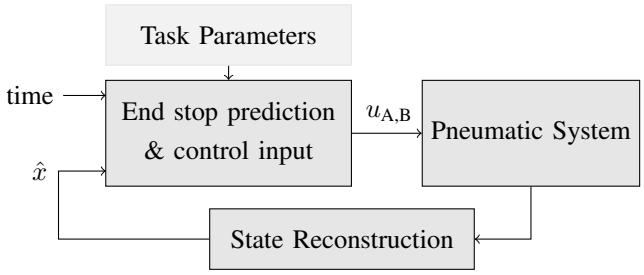

Fig. 7. Block Diagram of the proposed control scheme in Section III-D.

i.e. the MPC-prediction tells that the motion task will be fulfilled with $u_A = 0$, the supply air is shut off by the MPC-controller – just as the presented predictive control scheme does. However the proposed scheme achieves this switching with a simple forward simulation instead of an optimization.

The result of this end stop prediction is a supply air shutoff just as in the previously explained feed-forward case. Hence, we do not give a separate simulation example, but refer to the illustration of the feed-forward supply air shutoff in Fig. 6. The results of the control will be discussed in the next section together with our experiment.

IV. Experimental Results

A. Experimental Setup

Our experimental setup is illustrated in Fig. 1 in the introduction section. It contains a double stroke pneumatic cylinder with a diameter of $32\mathrm{mm}$, where both chambers are actuated by separate control valves. The sensing, actuating, as well as calculations are performed on a dSpace rapid control prototyping hardware.

B. Results

The experimental results of the two presented optimized control strategies are depicted in Fig. 8. For the strict feed-forward strategy from Section III-C, the optimal switching point was calculated offline, and the resulting system input was then applied. The corresponding time behavior is illustrated in Fig. 8 in blue color. The results from the end stop prediction of Section III-D are plotted in gray color. For the prediction, a discretization via Euler method with a step size of $1\mathrm{ms}$ was performed. The fourth sub-figure of Fig. 8 illustrates the predicted end position at time T_f – and as soon as the end stop is expected to be reached, the supply air is shut off. Both control strategies result in a strong decrease of compressed air consumption: 1.41 standard liters is the consumption using the feed-forward strategy, and 1.26 standard liters in the predictive case. This is a decrease of 44.4%, and 49.4% respectively, compared to the original consumption of 2.49 standard liters as illustrated in the beginning of the paper.

The predictive solution shuts off the supply pressure earlier compared to the offline solution – this is a possible consequence of model errors, especially from the friction model. Hence, the predictive solution arrives at a lower

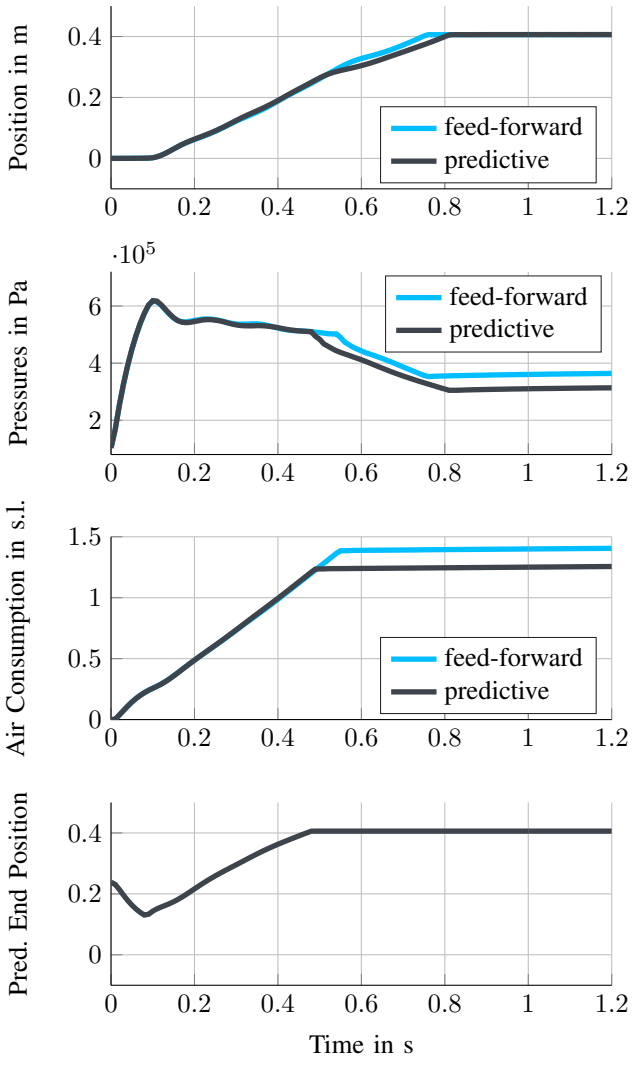

Fig. 8. Experimental results for the two proposed control strategies. The feed-forward optimal switching strategy is plotted in blue color and the measurements coming from the application of the end stop prediction are given in gray color ("predictive"). Both strategies result in a significant decrease of compressed air intake compared to the standard control (roughly one half, see Fig.2). The fourth plot illustrates the predicted end position $\hat{s}(T_\mathrm{F})$. Once it indicates the task will be fulfilled, the supply air is shut off.

compressed air consumption. Another benefit is that in case of the predictive solution, the control valve could be opened again in case the prediction tells the end stop will not be reached in the requested transition time. This would increase the energy intake, but ensure a proper transition time.

Note that the case where – in addition to the transition time – a force at stroke end is requested could also be taken into account by predicting the corresponding force at stroke end, and shutting off the supply air as soon as both boundary conditions are fulfilled.

V. Conclusions

We have investigated the energy intake of a pneumatic cylinder under different control strategies for a switching valve. To do so, we presented a mathematical model, identified the necessary parameters, and validated it in an experiment. We then derived a feed-forward strategy based on the optimal switching time for the control valve in order to fulfill the requested motion task, and a predictive strategy using a model-based online prediction of the cylinder's behavior and a control input based on this prediction.

The two strategies were implemented in an experiment and compared to one another. Both strategies reduce the energy intake of the pneumatic cylinder by about one half compared to the standard control strategy. The predictive strategy reveals slight advances over the feed-forward strategy. Furthermore, the proposed predictive scheme is easier to implement, and it is more robust with respect to changing parameters or initial conditions than the feed-forward strategy.

Further work should include the investigation of the system behavior in different scenarios, such as vertical motions or asymmetric load scenarios. In addition, it is worth to investigate which control heuristics could be derived from those results in different applications in order to pass by an optimization in actual application processes.

References

[1] A. Hildebrandt, R. Neumann, and O. Sawodny, "Optimal system design of siso-servopneumatic positioning drives," *IEEE Transactions on Control Systems Technology*, vol. 18, no. 1, pp. 35–44, 2010.

[2] M. Doll, R. Neumann, and O. Sawodny, "Dimensioning of pneumatic cylinders for motion tasks," *International Journal of Fluid Power*, vol. 16, no. 1, pp. 11–24, 2015.

[3] X. Shen and M. Goldfarb, "Energy saving in pneumatic servo control utilizing interchamber cross-flow," *Journal of Dynamic Systems, Measurement, and Control*, 2007.

[4] J. Parkkinen and K. Zenger, "A new efficiency index for analysing and minimizing energy consumption in pneumatic systems," *International Journal of Fluid Power*, vol. 9, no. 1, pp. 45–52, 2008.

[5] J. Hepke and J. Weber, "Energy saving measures on pneumatic drive systems," in *13th Scandinavian Conference on Fluid Power*, 2013.

[6] J. Ke, J. Wang, N. Jia, L. Yang, and Q. H. Wu, "Energy efficiency analysis and optimal control of servo pneumatic cylinders," in *IEEE Conference on Control Applications*, 2005, pp. 541–546.

[7] J. Wang and T. Gordon, "Energy-efficient tracking control of pneumatic cylinders," in *IEEE Conference on Decision and Control*, 2011.

[8] M. Doll, R. Neumann, and O. Sawodny, "Energy efficient use of compressed air in pneumatic drive systems for motion tasks," in *Conference on Fluid Power and Mechatronics*, 2011, pp. 340–345.

[9] M. Doll, O. Sawodny, and R. Neumann, "Energy efficient adaptive control of pneumatic drives with switching valves," in *8th International Fluid Power Conference*, 2012.

[10] A. Pfeffer, T. Glück, and A. Kugi, "Soft landing and disturbance rejection for pneumatic drives with partial position information," in *7th IFAC Symposium on Mechatronic Systems*, 2016, pp. 559–566.

[11] O. Ohligschläger, "Pneumatische zylinderantriebe - thermodynamische grundlagen und digitale simulation," Ph.D. dissertation, RWTH Aachen, 1990.

[12] E. Richer and Y. Hurmuzlu, "A high performance pneumatic force actuator system: Part i - nonlinear mathematical model," *Transactions of the ASME*, vol. 122, pp. 416–425, 2000.

[13] B. M. Y. Nouri, F. Al-Bender, J. Swevers, P. Vanherck, and H. V. Brussel, "Modelling a pneumatic servo positioning system with friction," in *American Control Conference*, 2000, pp. 1067–1071.

[14] *Pneumatic fluid power - Determination of flow-rate characteristics of components using compressible fluids*, ISO 6358 Std.

[15] F. E. Sanville, "A new method of specifying the flow capacity of pneumatic fluid power valves," in *BHRA 2nd International Fluid Power Symposium*, 1971.

[16] D. Bertsekas, *Nonlinear Programming*. Athena Scientific, Belmont, Massachusetts, 2006.

[17] J. T. Betts, *Practical methods for optimal control and estimation using nonlinear programming*. Siam, 2010.